

# Ionic Naphthalene Thermotropic Copolyesters: Effect of Ionic Content

Yongpeng Xue and Masanori Hara\*

Department of Chemical & Biochemical Engineering, Rutgers University,  
Piscataway, New Jersey 08855-0909

Received November 19, 1996; Revised Manuscript Received March 15, 1997<sup>o</sup>

**ABSTRACT:** Ionic naphthalene thermotropic polymers (NTP) based on wholly aromatic (main chain liquid crystalline) copolyesters were prepared, in which ionic monomer was introduced in the form of sodium 5-sulfoisophthalate. This meta-linked monomer introduces ionic groups as well as “kinked” units into polymer chains. A fiber-forming molecular weight was achieved for all the ionic NTP. The melt of ionic NTP showed extensive birefringence, and the majority of them exhibited nematic mesophase textures over a wide temperature range, without showing a transition to an isotropic phase at least up to 380 °C. The melting temperature ( $T_m$ ) and the crystallization temperature ( $T_c$ ) of the ionic NTP are both decreased substantially with an increase in ion-containing monomer content because of an increase of the number of “kinked” units. A unique glass transition behavior is also observed: at the ionic content of less than 10 mol %, the glass transition temperature ( $T_g$ ) is rather constant, the  $T_g$  value jumps when the ionic content reaches 15 mol %, and two distinct  $T_g$ 's with ca. a 40 deg separation are observed at 20 mol % ionic content. This seems to arise from the competition between two opposing factors: one is a reduction of the rigidity of backbone chains by “kinked” units, which leads to lower  $T_g$ , and another is intermolecular ionic interactions between chains, which lead to higher  $T_g$ . Fracture surfaces of the ionic NTP fibers indicate suppression of spontaneous fibrillation with an increase of ionic content. This is an indication of decreased rigidity of the backbone chains and increased cohesion through ionic interactions between the polymer chains. Also, flat fracture surfaces observed for the high ionic content NTP fibers reflect their brittleness, arising from easier crack propagation.

## Introduction

Liquid crystalline polymers (LCPs) have been actively studied recently because of their technological potential and scientific challenges.<sup>1–3</sup> LCPs contain inherently rigid units, thereby forming a highly “extended chain” morphology, leading to remarkable mechanical properties and thermal stability. For example, some fibers made by these polymers compete with the best ceramic fibers and are far superior to metal fibers.<sup>4</sup> There are two major LCP types: one is lyotropic LCP, e.g., Kevlar based on poly(*p*-phenyleneterephthalamide) (PPTA),<sup>5</sup> which forms a liquid crystalline structure with a diluent (in solution); another is thermotropic LCP, e.g., Vectra based on wholly aromatic polyester,<sup>6</sup> which forms a liquid crystalline structure upon heating. While the lyotropic LCP can be fabricated only in fibers or films, the thermotropic LCP can be made into a three-dimensional structure by conventional processing, such as injection molding. This makes thermotropic LCP a unique material for a wide range of applications.<sup>7</sup> As summarized by Yoon et al., the motivation for the development of thermotropic liquid crystalline polymers (TLCPs) has been the establishment of a cost-effective technology for high-performance engineering resins and high-strength, high-modules fibers.<sup>8</sup>

Although LCPs have been widely used as high-performance polymers, two major problems prevent their extensive use. One is poor transverse and compressive properties in contrast to very high axial properties, often 1–2 orders of magnitude lower, both of which are inherent to highly uniaxially oriented polymers.<sup>2</sup> Another problem is poor miscibility and adhesion with other polymers, when LCPs and conventional polymers are mixed to produce polymer blends,

which are widely used to enhance polymer properties.<sup>9,10</sup> Both problems basically arise from weak intermolecular interactions either in the LCP itself or in an LCP/polymer blend.<sup>2</sup> These interactions are usually weak secondary bonds (van der Waals bonds and hydrogen bonds), in contrast to strong covalent bonds along chain directions. These problems hinder the development of LCPs into a wide range of applications, including conventional composites.<sup>7</sup>

We are currently developing ionic LCPs to overcome these fundamental problems by introducing ionic groups into LCP molecules. Strong ionic interactions between polymer molecules are known to significantly enhance mechanical properties, which include compressive strength,<sup>11,12</sup> as demonstrated for flexible ionomers,<sup>13</sup> and also known to dramatically improve compatibility between different polymers in polymer blends.<sup>14–17</sup> Therefore, ionic LCP should have higher transverse/compressive strength and better compatibility with many (polar) polymers (including many engineering polymers) than unmodified LCPs.

It is also of interest to investigate how the ionic interactions modify liquid crystallinity, liquid crystalline structure, and overall morphology of the LCP. As a base polymer of ionic LCPs, we have chosen wholly aromatic polyesters based on random copolymers of 1,4-hydroxybenzoic acid (HBA) and 6,2-hydroxynaphthoic acid (HNA), one example of so-called *naphthalene thermotropic polymers* (NTPs).<sup>18</sup> Incorporation of naphthalene-based units (e.g., HNA) reduces  $T_m$  very effectively without losing excellent mechanical and thermal properties. This polymer was first commercialized in the mid-1980s as the Vectra series.<sup>19</sup> These polymers possess desirable properties, such as high mechanical strength and stiffness, high-temperature performance, chemical resistance, dimensional stability, and ease of processing.<sup>8,18–23</sup> However, like other LCPs, these materials show rather poor mechanical properties in the

\* To whom all correspondence should be addressed.

<sup>o</sup> Abstract published in *Advance ACS Abstracts*, June 1, 1997.

**Table 1. Composition of Feed Monomers (mol %) for Ionic and Nonionic NTP**

sample no.	HBA	HNA	SSI	HQ
A	74	26	0	0
B	73	26	1	0
C	70	26	2	2
D	64	26	5	5
E	60	26	7	7
F	54	26	10	10
G	44	26	15	15
H	34	26	20	20

transverse direction in contract to the longitudinal direction, again due to weak intermolecular interactions.<sup>2</sup> By comparing the theory of the strength of LCP fibers with the experimental results of the strength (or tenacity) of Vectra fibers, Yoon has pointed out that intermolecular adhesion between the LCP chains is relatively weak and that any process that increases the shear strength (as a result of enhanced intermolecular adhesion) will also increase the fiber strength.<sup>24</sup> Thus, incorporation of ionic groups may also lead to better tensile strength.

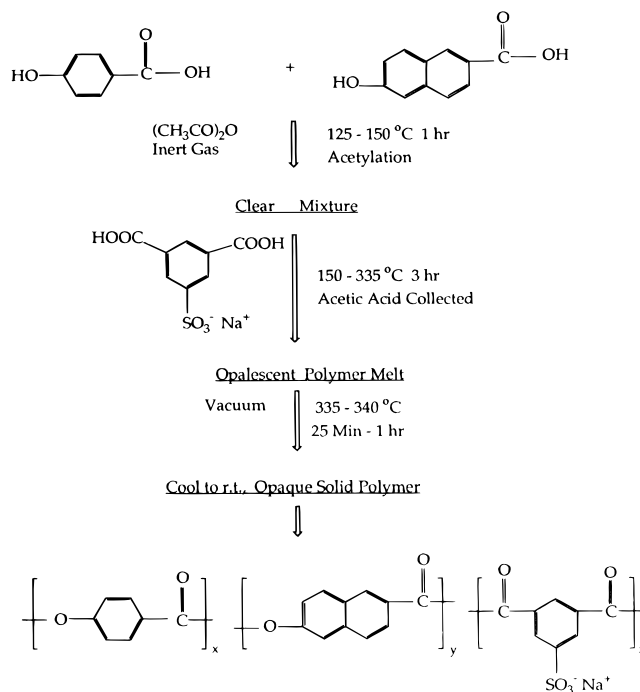
As an ion-containing unit in ionic LCPs, we have chosen *sodium 5-sulfoisophthalate*. The incorporation of this unit into the polymer chain introduces ionic bonds between polymer chains. In addition, this meta-linked monomer introduces "kinked" units into the backbone chains; therefore, they are expected to further reduce the melting (and processing) temperature of NTP polymers. Shepherd et al. reported that the addition of a small amount of such ionic moieties to the backbone of wholly aromatic LCPs (NTPs) improved the adhesion properties of the resulting polymers.<sup>25</sup> However, little information is available about their structure and properties, and specifically the effect of ionic interactions. Therefore, we have decided to conduct a more systematic investigation on the ionic NTPs.

In this article, the first one of the series on ionic NTPs, we report initial results on synthesis and characterization of ionic NTPs based on wholly aromatic copolyesters (NTP). Thermal analysis, polarizing light microscopy, scanning electron microscopy (SEM), and FTIR are used to investigate their thermal properties, optical textures, fracture morphology, and local structures. Emphasis is placed on obtaining an overall picture of the effect of ion-containing units on these properties. Results on the mechanical properties of these polymers will be reported separately in a subsequent paper.<sup>26</sup> Also, results concerning ionic NTPs that contain different types of ion-containing monomers will be reported.<sup>27</sup>

## Experimental Section

**Materials.** 4-Hydroxybenzoic acid (HBA, 99%, mp 215–217 °C), hydroquinone (HQ, 99+%, mp 172–175 °C), sodium 5-sulfoisophthalate (SSI, and acetic anhydride (99.2%, bp 138–140 °C) were purchased from Aldrich Chemical. 6-Hydroxy-2-naphthoic acid (HNA, 99.5%, mp 248–250 °C) was provided by Hoechst Celanese. All the materials were used as received without further purification. The purity of the monomers was tested by purity analysis on DSC before use.

**Synthesis of Ionic NTP Polymers.** All the copolyesters, run on a scale of 0.1 mole of base monomers, were prepared from part or all of the monomers depending on their compositions (see Table 1). Polymerization reactions, as indicated in Figure 1, were carried out by melt acidolysis based on a procedure described by Shepherd et al.<sup>25</sup> Monomers were charged into a round-bottomed three-neck flask, equipped with a spherical adaptor leading to a water-cooled condenser, a graduated cylinder, a nitrogen gas inlet, a heater, and a mechanical stirrer (a glass rod with a stainless steel paddle).

**Figure 1.** Synthesis scheme of ionic NTP.

An attachment for application of vacuum was provided at the end of the condenser. Acetic anhydride was introduced into the flask, which was purged with a strong stream of dry nitrogen gas. A 2.5 mol % excess of anhydride (to hydroxy functionality) was added to ensure complete acetylation of the monomers. Above 1 mol % SSI content, HQ monomer was added to balance the extra carboxy group of the SSI monomers, whose concentration increases with ionic moiety. All the condensation reactions were carried out by an *in situ* acetylation procedure; i.e., the hydroxy groups of the monomers reacted with carboxy groups in the presence of acetic anhydride, which acted as an acetylating agent as well as a condensation agent. Because the ionic monomer would act as catalyst, no extra catalyst was added to any of the compositions except to sample A, in which potassium acetate corresponding to a 0.01 wt % of monomers was added as catalyst.

The general reaction procedure was as follows. First, the monomer mixture was heated, under stirring with high-purity nitrogen gas flow, from room temperature to 340 °C via different temperature–time cycles: i.e. from room temperature to 125 °C as quick as possible (about 25 min), from 125 to 140 °C over 40 min, from 140 to 150 °C over 20 min, from 150 to 200 °C over 45 min, from 200 to 335 °C over 2 h 15 min, from 335 to 340 °C over 10 min, and at 340 °C for 15 to 50 min. Vacuum was applied at the last reaction stage. The reaction was monitored through the volume of acetic acid that distilled out. An increase in viscosity of the reaction mixture was noted at above 200 °C when polymer began to be formed. After 90 vol % acetic acid was distilled out, the pressure of the reaction system was reduced gradually until full vacuum was reached. During this period, the viscosity of the polymer melt continued to increase while the remaining acetic acid was distilled out. All the polymers eventually achieved a fiber-forming molecular weight; this was tested by drawing a fiber directly from the melt with a spatula. Heating was terminated when no further acetic acid was distilled out. The polymer melt was then allowed to cool to ambient temperature. When the SSI monomer content exceeded 10 mol %, 15–20 mL of DMF was added at the beginning of the reaction to make the SSI monomer more miscible with other monomers during the reaction, and the maximum reaction temperature was reduced to 270 °C. Polymers were collected by breaking the cooled flask, then ground into a fine powder in a freeze mill, and vacuum dried at 120 °C for 24 h. Ionic NTP samples were stored in a desiccator with drying agent.

**Measurements.** Infrared (IR) spectroscopy measurements were made using an ATI Mattson (Genesis Series FTIR) spectrometer with average scan of 25 at a resolution of  $2\text{ cm}^{-1}$  in a transmission mode. The films for IR measurements were made either by extrusion or compression molding. Low ionic content NTP films (0 and 1 mol % ionic content) were made by melt extrusion using a Micro-Melt extruder (Hoechst Celanese) with a film die of 0.005 in. thickness and 0.250 in. width. The melt-extruded film, cooled at ambient temperature and collected by a take-up roll with a take-up speed of 5 m/min, had a film thickness of  $30\text{ }\mu\text{m}$  on average. High ionic content NTP films (2–7 mol % ionic content) were made through compression molding at 24 000 psi using a Carver Laboratory Press (Model 2699) by sandwiching the powder samples between two plates of the press machine. The resultant films from compression molding had an average thickness of  $20\text{ }\mu\text{m}$ .

Thermal transitions of the polymers were studied by differential scanning calorimetry (DSC) using a TA Instrument thermal analyst (2100/910). Samples of 5–10 mg were examined at a heating rate of  $20\text{ }^{\circ}\text{C}/\text{min}$ , followed by cooling to ambient temperature under a nitrogen atmosphere, to determine the glass transition, melting, and crystallization temperatures ( $T_g$ ,  $T_m$ , and  $T_c$ ). The  $T_g$  is taken from the midpoint between the onset and the end point of the step transition region, and  $T_m$  and  $T_c$  are taken from the peak temperatures of the melting endotherm and crystallization exotherm on DSC thermograms. The thermal stability of ionic NTP samples was tested by thermogravimetric analysis (TGA) using a TA Instrument (2100/951). Samples of ca. 15 mg were tested at a heating rate of  $10\text{ }^{\circ}\text{C}/\text{min}$  under a nitrogen atmosphere.

The sample for polarizing light microscopy was prepared by heating a small amount of polymer powder sandwiched between a microscope glass slide and a cover glass on a hot-stage (Mettler F52) to a temperature a few degrees above its melting temperature or to a temperature ca. 100 deg above its glass transition temperature for a sample showing no melting temperature, followed by applying a manual shear force to make a thin film appropriate for viewing. The thin film was reheated to the same temperature as that used for initial heating and examined under a polarized microscope (Leitz, Ergolux). The image was retained for all the samples after being quenched to ambient temperature. Thus, the polarized light micrographs of all samples were taken at room temperature with a polarized light microscope (Olympus, BH-2) using Polaroid 59 film, which allowed desirable color image and magnifications.

The morphological characteristics of the fiber samples of ionic NTP were examined by scanning electron microscopy (SEM). The fiber was made by drawing directly from the hot melt with a thin glass rod and quenching in air. The SEM specimens were fractured in air, mounted on a stub with conducting double-sided carbon tape, and coated with gold in a sputter coater (Polaron, SEM coating unit E5100) for 4 min. They were examined with a scanning electron microscope (Amray 1200C) operating at 30 kV, and images were recorded directly from the cathode ray tube on Polaroid 55 films.

## Results and Discussion

**Initial Characterization of Ionic NTPs.** To show that ionic groups are successfully incorporated into NTP chains, some FTIR and elemental analyses were used. IR absorption bands are well-known for their marked specificity to individual chemical functionalities. However, the assignment of IR absorption bands for specific modes of molecular vibration in polymers is not always straightforward, since IR bands can be affected by various factors, such as sample history, IR sampling techniques, phase, and morphology.<sup>28</sup> Despite these limitations, IR spectroscopy still can provide useful information on characterization of TLCPs.<sup>29,30</sup> Also, characteristic bands corresponding to the sulfonate group in polymers have been analyzed by IR spectroscopy, as recently reported for sulfonated polystyrenes and their blends.<sup>31,32</sup> Thus, we have applied the IR

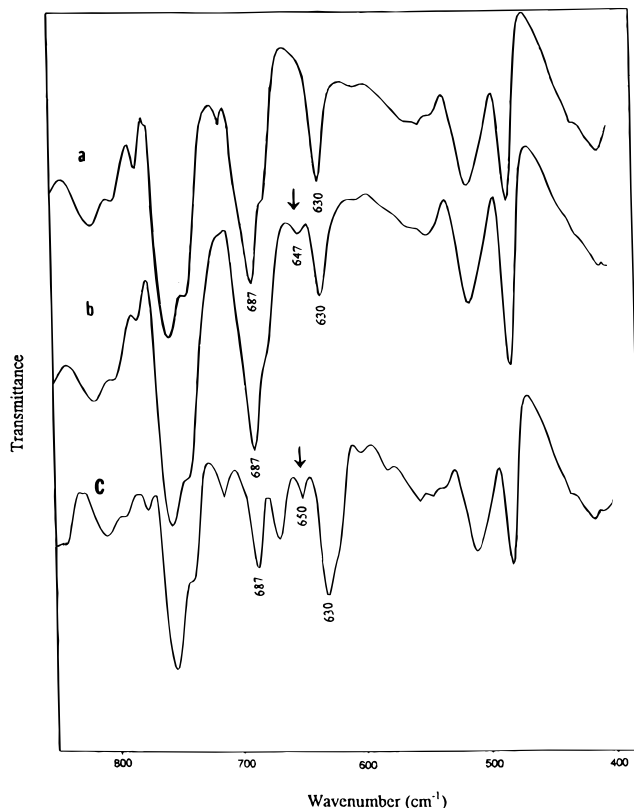


**Figure 2.** IR spectra for (a) nonionic NTP, (b) 1 mol % ionic NTP, and (c) 7 mol % ionic NTP in the range of 400–850  $\text{cm}^{-1}$ .

technique to the ionic NTP system. We chose two representative ionic NTP samples as well as a nonionic NTP sample: one is a 1 mol % sample, representing low ionic content samples that show only melting and no glass transition; another is a 7 mol % sample, representing higher ionic content samples that show a clear glass transition.

In a spectrum of the nonionic NTP film, the IR absorption bands of the C=O stretching vibration ( $1734$ ,  $1752\text{ cm}^{-1}$ ), a weak band due to the overtone of the C=O stretching vibration of the ester linkage ( $3454\text{ cm}^{-1}$ ), and a band of aromatic stretching vibrations ( $3075\text{ cm}^{-1}$ ) are clearly identified. A major difference between ionic NTP and nonionic NTP is that the former contains ionic sulfonate groups and the latter does not. For organic sulfonic acid salts, the IR absorption range of the O=S=O asymmetric and symmetric stretching modes lies in  $1150$ – $1260$  and  $1010$ – $1080\text{ cm}^{-1}$ , respectively, and that of the S–O stretching mode lies in  $600$ – $700\text{ cm}^{-1}$ .<sup>33</sup> Because of the overlap found for both asymmetric and symmetric stretching bands of  $\text{SO}_2$  with ester C–O stretching bands in the polymers under study, the S–O stretching mode is chosen for identification of sulfur groups in the ionic NTP. Figure 2 compares the IR spectra in the range of  $400$ – $850\text{ cm}^{-1}$  for (a) nonionic NTP, (b) 1 mol % ionic NTP, and (c) 7 mol % ionic NTP. While there is no S–O stretching mode found in nonionic NTP, such a mode is found as a weak band at  $647\text{ cm}^{-1}$  for the sample of 1 mol % ionic content, and a stronger absorption band is found at  $650\text{ cm}^{-1}$  for the sample of 7 mol % ionic content. These results clearly indicate successful incorporation of ionic (sulfonate) groups, whose concentration increases with an increase in the concentration of SSI monomers in the feed.

Also, the number-average molecular weight,  $M_n$ , of three representative samples (with ionic contents of 0,

1, and 7 mol %) was determined by end-group analysis via IR spectroscopy.<sup>25,34</sup> The analysis was conducted as follows. A weak absorption around  $3003\text{ cm}^{-1}$  was assigned to a methyl band of the acetoxy end groups, and absorptions at  $3075\text{--}3106\text{ cm}^{-1}$  were assigned to the aromatic CH bands of the polymer backbone. The absorbances at the wave numbers indicated above were determined by integration of peak areas from the same spectrum using spectral manipulation software. The equation  $A = xcd$ , where  $A$  is the absorbance,  $x$  is the molar absorption coefficient,  $c$  is the concentration, and  $d$  is the sample thickness, was used to estimate the relative concentration of the aromatic C—H of the polymer backbone and the aliphatic C—H of the acetoxy end groups. Here, the molar absorption coefficients for the aromatic CH band and the aliphatic CH band were evaluated from calibration graphs of IR vibrational spectra for several aromatic and aliphatic compounds.<sup>35</sup> The number-average molecular weight,  $M_n$ , was then estimated from the ratio of the relative concentrations. The  $M_n$  values of nonionic NTP and two ionic NTPs are in the range 5000–7000. These results are consistent with the observation that all the ionic and nonionic NTPs prepared led to fiber formation, drawn manually from the melt, which needs a reasonable molecular weight.

In addition, to check if proper amounts of ionic groups were incorporated into the NTP chains, elemental analysis was carried out for two representative samples; i.e., samples having 1 and 5 mol % ionic contents (performed by Robertson Microlit Laboratories). The results are as follows: (a) Calcd for 1 mol % sample: C, 71.86; H, 3.39; S, 0.24; Na, 0.17. Found: C, 71.36; H, 3.03; S, 0.22; Na, 0.15. (b) Calcd for 5 mol % sample: C, 69.62; H, 3.26; S, 1.21; Na, 0.87. Found: C, 68.48; H, 3.14; S, 1.18; Na, 0.85. The experimental data are in good agreement with the calculated values, showing again successful incorporation of proper amounts of ionic groups into the NTP chains.

#### Effect of Ionic Content on Thermal Properties.

It is well-known that the incorporation of ionic groups leads to an elevated glass transition temperature for ionomers based on amorphous, flexible polymers, such as polystyrene.<sup>11–13</sup> Also, for ionomers based on crystalline, flexible polymers, such as polyethylene,<sup>36,37</sup> ionic incorporation leads to decreased crystallinity for quenched specimens, but the value will rise to the level of the nonionic base polymer after annealing. In addition, the incorporation of meta-linked “kinked” units is expected to decrease  $T_m$ , as reported for LCP polymers,<sup>38</sup> and to decrease  $T_g$  by reducing the rigidity of the polymer chains. Thus, it is of interest to study how the incorporation of ion-containing, meta-linked monomer modifies these transition temperatures.

Primary transitions to be discussed here are melting (three-dimensional solid crystal to nematic liquid melt), crystallization, and glass transition. A temperature range covering these transitions of NTP and ionic NTPs is far above the room temperature, as seen in Figures 3 and 4: Figure 3 shows heating curves and Figure 4 shows cooling curves in the DSC thermograms, which are plotted on the same scale of the heat flow to show the changes associated with the change in the ionic content. The shape and the position of the melting peak for the nonionic NTP are in very good agreement with those reported.<sup>39</sup> Figure 3 also indicates that the melting temperature, which is taken from the maximum peak temperature, decreases with increasing ionic

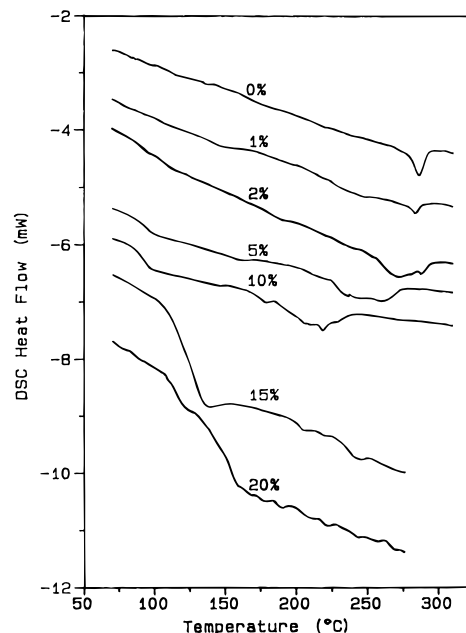


**Figure 3.** DSC thermograms (heating curves) of ionic NTPs with different ionic contents (mol %).

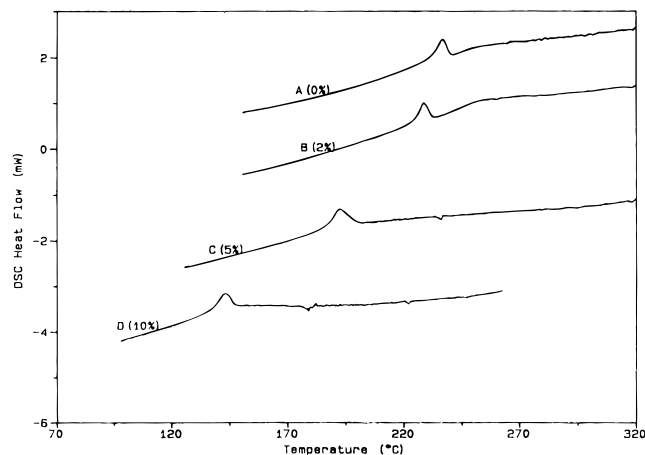


**Figure 4.** DSC thermograms (cooling curves) of ionic NTPs with different ionic contents (mol %).

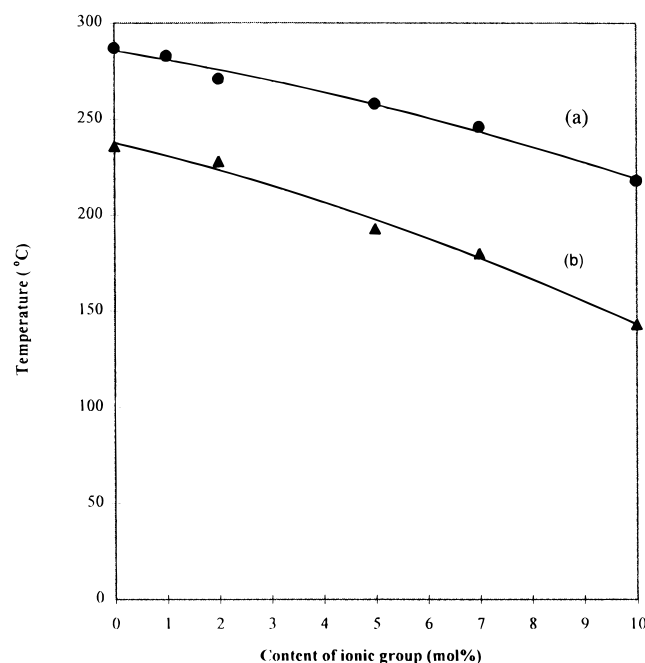
content and no melting is identified above 15 mol % ionic content. The figure also shows that a glass transition begins to appear at 5 mol % and a step (change in the specific heat between before and after the transition) becomes larger with ionic content. Exothermic crystallization peaks are also shifted to lower temperatures as the ionic content increases, as seen from Figure 4. Transition temperatures ( $T_m$ ,  $T_g$ ,  $T_c$ ) and the heat of fusion ( $\Delta H_m$ ) determined from these curves are listed in Table 2.

Figure 5 shows how the melting temperature and the crystallization temperature change with ionic content: both the  $T_m$  and  $T_c$  decrease substantially with ionic content up to 10 mol %. This is because the ionic monomer is a meta-linked phenylene ring with a pendant ionic group; and, the incorporation of such “kinked” units in random position into the rigid polymer chains reduces the melting temperature greatly. The introduction of such “kinked” units into LCP chains is considered to be a useful method in reducing melting temperature, thus also the processing temperature.<sup>2</sup> For example, the copolymer reported by Siemionko<sup>38</sup> has the same structure as our copolymer except our LCP has ionic groups attached to the “kinked” units; these

**Table 2. DSC Results for Ionic and Nonionic NTP**

sample no.	ionic content (mol %)	$T_g$ (°C)	$T_m$ (°C)	$T_c$ (°C)	$\Delta H_m$ (J/g)
A	0	— <sup>a</sup>	286	236	4.8
B	1	—	283	# <sup>b</sup>	0.9
C	2	—	271	228	3.4
D	5	95	258	193	3.4
E	7	96	246	180	3.1
F	10	92	218	143	3.5
G	15	127	—	—	—
H	20	115, 153	—	—	—

<sup>a</sup> Not detected. <sup>b</sup> Difficult to detect.



**Figure 5.** (a) Melting temperature and (b) crystallization temperature against ionic content for ionic NTPs.

nonionic NTPs show a decreasing tendency in  $T_m$  with an increase in the number of "kinked" units. We also have preliminary data on ionic NTPs containing "straight" ionic units instead of the "kinked" units, which show no drop in  $T_m$ ,<sup>27</sup> thus supporting our reasoning that the reduction in  $T_m$  comes from "kinked" units and not from ionic interactions. This is further substantiated by the known effect of ionic interactions on the  $T_m$  of polyethylene ionomers: ionization has little effect on the melting behavior of the acid copolymer, poly(ethylene-*co*-methacrylic acid), a precursor of polyethylene ionomer.<sup>37</sup> The drop of  $T_c$  is reasonable, since the destruction of chain periodicity inhibits crystallization markedly, reducing the crystallization temperature, as reported for other LCPs.<sup>2</sup> These results, showing a gradual decrease in  $T_m$  and  $T_c$  with ionic content, also demonstrate that the proper amounts of ion-containing "kinked" units are indeed incorporated into the NTP chains.

An increased broadening of melting peaks with an increase in the ionic content is seen from the normalized (with respect to the total heat flow) DSC thermograms (see Figure 3). These results should reflect increased diversity in size and in the arrangement of crystallites, possibly due to increased structural heterogeneity in these ionic NTPs. However, the heat of fusion remains essentially constant for the majority of samples ( $\Delta H_m$  of 0–10 mol % samples in Table 2), which indicates no significant change in crystallinity. Extensive study was conducted on a polyethylene-based ionomer, poly-

(ethylene-*co*-sodium methacrylate), better known as Surlyn; it is demonstrated that the crystallinity is virtually independent of the ionic content for annealed samples, although quenched specimens have a smaller degree of crystallinity.<sup>36</sup> Since our DSC results shown are taken either from the second or third run after heating to over 300 °C, annealing was achieved; thus, the nearly constant crystallinity, a 10–20% range determined by X-ray diffraction for nonionic NTP,<sup>39</sup> is consistent with the results on polyethylene ionomers. It should be added that translucent polyethylene films turn clear upon introduction of ionic groups, reflecting the change in spherulite structures—smaller spherulites or even lamellar structures.<sup>36</sup> We may expect a similar situation for the ionic NTPs: the size and order of the crystalline structure are different from those in the nonionic NTP.

The effect of ionic content on glass transition temperatures of ionic NTP is seen from Figure 3 and Table 2. At lower ionic content (2 mol % and below), no glass transitions are detected by DSC measurements. The transition becomes visible when the ionic content reaches 5 mol % and becomes more apparent at higher ionic contents. Below 10 mol % ionic content,  $T_g$  values are very close, but a sharp increase (over 30 °C) is seen at 15 mol % ionic content. These results differ from conventional ionomers based on flexible chains, such as polystyrene-based ionomers and poly(methyl methacrylate)-based ionomers: all of them exhibit a nearly linear increase of  $T_g$  with an increase of ionic content.<sup>12,40,41</sup> This difference is interesting because, in ionic NTP, two major factors may compete with each other to affect glass transitions. First, the incorporation of "kinked" units, which contain ionic groups, reduces the rigidity of the polymer chain and, consequently, reduces the  $T_g$ . Second, the formation of ionic cross-links reduces the segmental mobility of the main chain, and as a result, the  $T_g$  rises.<sup>12</sup> As seen from Table 2, below 10 mol % ionic content, two competing factors seem to be balanced. At 15 mol % ionic content, the effect of ionic cross-links and interactions seems dominant. At 20 mol % ionic content, the  $T_g$  splits into two distinct transitions of about 40 deg difference. This may be explained in terms of the multiple-cluster model<sup>12,42</sup> used for conventional flexible ionomers. In this scheme, at lower ionic contents, ion pairs exist as small ionic aggregates, called multiplets, as well as isolated ion pairs. These multiplets work as ionic cross-links and raise the  $T_g$ . As the ionic content increases, an ion-rich "phase", called a cluster "phase", begins to form and increases its volume. The cluster "phase" is considered to be a separate phase having its own  $T_g$ , which is higher than that of the multiplet's  $T_g$ .<sup>42</sup> Therefore, at higher ionic content, two distinct  $T_g$ 's are observed for conventional ionomers. In ionic NTP of 20 mol % ionic content, where polymer chains become more flexible due to the higher percentage of "kinked" units incorporated, the lower glass transition may reflect a multiplet  $T_g$ , and the higher one may correspond to a cluster  $T_g$ , although DSC data only are not sufficient to prove the existence of multiplets and clusters conclusively.<sup>12,42</sup>

Thermal stability of NTP and ionic NTP samples was studied by thermogravimetric analysis (TGA). TGA curves for three representative NTP samples (with 5, 7, and 10 mol %) are shown in Figure 6. In these curves, the threshold temperature is defined as the temperature at which a deviation from the initial base line is noted; and, the onset point temperature is defined as the

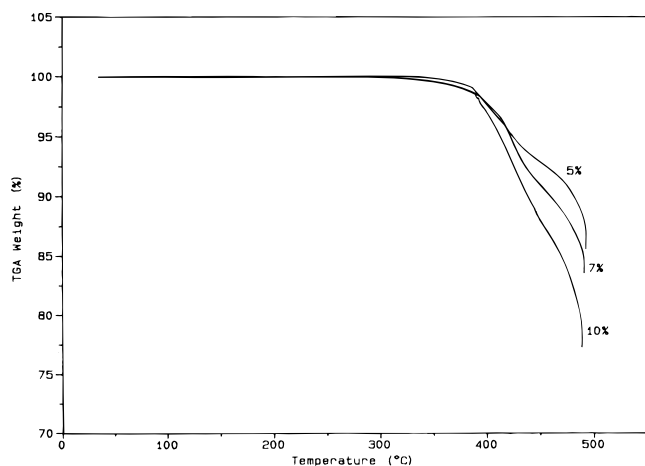


**Figure 6.** TGA curves of three ionic NTPs with ionic contents of 5, 7, and 10 mol %.

**Table 3.** TGA Results of Ionic and Nonionic NTP

sample no.	ionic monomer content (mol %)	threshold temp (°C)	onset point temp (°C)	10 wt % loss temp (°C)
A	0	326	383	479
B	1	329	386	487
C	2	305	385	489
D	5	313	383	483
E	7	316	382	460
F	10	308	383	439

temperature at which two tangential lines intersect. Before the onset point temperature, only minor weight loss (less than 1.5%) was noted. These temperatures for ionic NTPs are listed in Table 3. All the threshold temperatures are over 300 °C, indicating good thermal stability of ionic NTP samples. The onset temperatures are surprisingly close for all the samples, although the difference of ionic content is as large as 10 mol %: no significant weight loss is found up to 380 °C for all the samples in which crystallinity still remains. However, as seen from Figure 6, and also from the 10 wt % loss temperature in Table 3, after passing the onset point temperature, thermal degradation occurs more rapidly for ionic NTP having a higher ionic content. This probably arises from the loss of chain rigidity due to the incorporation of "kinked" units and to thermal degradation of sodium sulfonate groups at such high temperatures, as noted for sulfonated polystyrene ionomers.<sup>41</sup>

**Effect of Ionic Content on Optical Textures of Thin Films.** When ionic NTP powders are heated first above their melting temperatures between a glass slide and a cover glass, only a small portion (thin section) of the samples transmits light and exhibits birefringence (color image) with nematic threaded texture in fine scale, while a large portion (thick section) of the samples is opaque. The cover glass is then pressed down, along with a slight manual shear force, to form relatively homogeneous thin films. The polymer melts are optically anisotropic (i.e., they transmit light when examined under crossed polarizers), and the amount of light transmitted increases when the sample is sheared. However, it should be added that the sample is optically anisotropic even without applying shear. This is quite similar to the results reported on copolyesters that have similar structural formulas but have no ionic groups.<sup>38</sup>

All the ionic NTP films formed from the melt exhibit some degree of birefringence when examined under crossed polarizers (see Figure 7). One advantage of the TLCPs is that the structure of the liquid crystalline

state can be "frozen in" upon cooling and studied in solid samples.<sup>43</sup> The images of all samples examined under the crossed polarizers show no change upon heating to 380 °C<sup>44</sup> or cooling to ambient temperature. This allows us to record the image at higher magnifications by using a polarized light microscope at ambient temperature. No nematic-to-isotropic transition is observed for all the samples tested up to 380 °C, 90–160 deg above their melting temperatures depending on the sample (see Table 2). These results are also consistent with the DSC results, which show no such transitions on the thermograms before the thermal degradation temperature, e.g., the onset point of ca. 380 °C.

For 0–10 mol % ionic contents, even though all melt-quenched films exhibit nematic threaded textures under crossed polarizers, the size and patterns of these textures are different. The nonionic NTP sample reveals a more homogeneous structure that contains threadlike texture in a very fine scale (Figure 7a). This type of less clearly defined optical texture with a fine scale (of the order of 1  $\mu$ m) is well-known for main-chain thermotropic copolyesters.<sup>2</sup> As the ionic content increases, the randomness and size scale of textures increase (Figure 7b). This is presumably due to an increase in chemical and structural inhomogeneities associated with an increase of ionic monomer content. Parts c and d of Figure 7 show optical textures for the ionic NTP of 10 mol % ionic content: Figure 7c is the thick section of the film, which reveals a very dense threadlike texture, and Figure 7d shows the thin section of the film in which many individual lines and loops,<sup>45</sup> characteristic of nematic structures, are clearly revealed. The appearance is quite different due to the superposition of structures:<sup>46</sup> the thick section has a threadlike texture with little detail compared to the thin region. At the ionic content of over 10 mol %, crystallinity is frustrated, resulting in sharper glass transitions and absence of melting endotherms, as noted in Figure 3. However, this does not mean complete elimination of the mesophase. As shown in Figure 7e, many rectangular birefringent domains are dispersed in the isotropic melt even at 15 mol % ionic content. The size of these mesophase domains reduces substantially when the ionic content reaches 20 mol % (not shown). To explain these changes of optical textures, the biphasic behavior<sup>47,48</sup> of LCPs should be considered. Biphasic behavior reflects the presence of two distinct phases, a mesophase and an isotropic melt, between the melting and clearing (or upper transition) temperatures. Martin and Stupp reported that a biphasic region becomes broad by as much as 120 deg for chemically disordered LCPs as compared with a narrow range of 5 deg for chemically ordered LCPs.<sup>48</sup> Since the disordered LCPs are made by random copolymerization, they have chemical heterogeneity. This is the same for our system: as the ionic content increases, the chemical heterogeneity increases, leading to a larger degree of biphasic behavior.

Another observation made is the trace of shear direction in large-scale optical textures. For the non-ionic NTP, the lines following the shear direction are clear and almost parallel (Figure 7a). With an increase of ionic content from 1 to 2 and 5 mol %, the overall texture shows the direction of shear, although less clear and nonparallel lines are seen (Figure 7b). At 10 mol %, the thick section does not reveal any such direction, while the thin section shows the direction of shear. Finally, at 15 and 20 mol %, no trace of shear direction

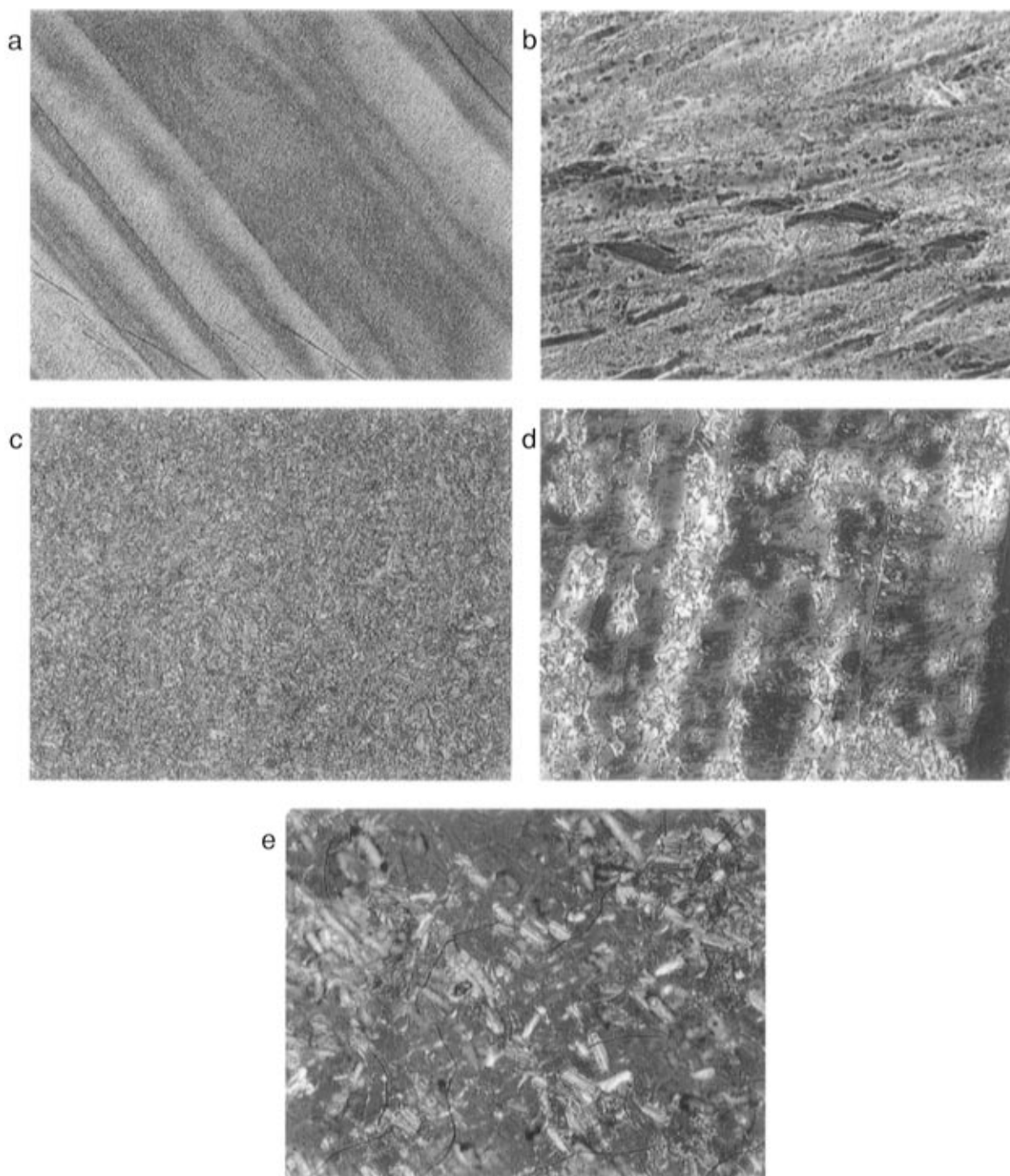


**Figure 7.** Polarized light micrographs (magnification  $\times 400$ ) of the ionic NTPs with different ionic contents: (a) 0 mol %; (b) 2 mol %; (c) 10 mol % (thick region of the film); (d) 10 mol % (thin region of the film); (e) 15 mol % (purple red color arises from the background due to the compensator used, and the isotropic phase also shows this color). Figure reduced to 66% for publication.

is noted. These changes are explained in terms of the reduction in the rigidity of the backbone chains and thus liquid crystallinity. When the polymer chains are still semirigid and liquid crystalline, there is a tendency for them to align along the shear direction, leading to the trace of the shear direction. Upon an increase in flexibility and a decrease of liquid crystallinity, the chains tend to follow the shear direction less, leading to the more isotropic structure. These observations are completely consistent with the changes in thermal behavior with ionic content, as already explained.

**Effect of Ionic Content on Fiber Fracture Surface and Skin Surface Morphology.** Scanning electron microscopy (SEM) is a useful tool for studying the morphology of TLCs.<sup>49–51</sup> It has been used extensively

in the investigations of fiber samples. In this study, the fibers were drawn manually from the polymer melts and were usually irregularly shaped. SEM micrographs in Figure 8 show both the fracture surface and skin surface of these fibers, and Figure 9 shows higher magnification scans of the fracture surfaces. In a general structural model for LCP extrudates and moldings, as well as for highly oriented fibrous materials, Sawyer and Jaffe<sup>52</sup> have shown various scales of microstructures ranging from macrofibrils (on the order of  $5\ \mu\text{m}$ ), to fibrils ( $0.5\ \mu\text{m}$ ), and to microfibrils ( $0.05\ \mu\text{m}$ ). According to this model, one can note the fibril structure in the fracture samples having an ionic content of 1–5 mol %. As an example, a layered structure with many fibrils is revealed clearly for the sample of 1 mol % ionic content



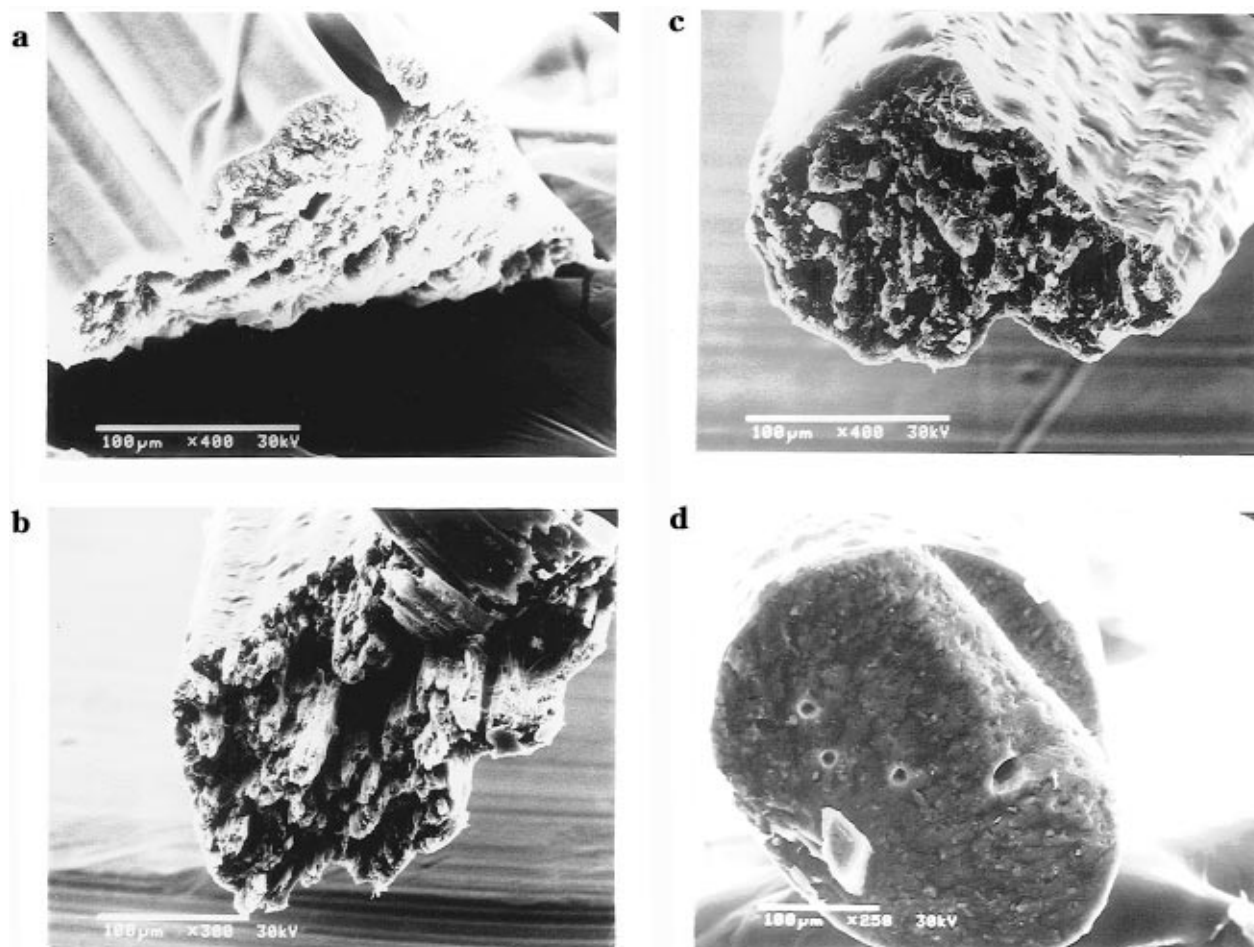


**Figure 8.** SEM micrographs showing fracture surfaces and skin surfaces of manually drawn ionic NTP fibers with different ionic contents: (a) 0 mol %; (b) 2 mol %; (c) 5 mol %; (d) 20 mol %.

(see Figure 9a). Both the size and the number of the fibrils are reduced significantly with an increase in ionic content. Eventually, samples with higher ionic contents (above 7 mol %) exhibit a more uniform dense fracture morphology without showing clear fibril structures, as typically seen for the sample with 10 mol % ionic content (Figure 9b). Plate<sup>53</sup> has described that the domain flow of the preparation, and the instability of the maximally oriented liquid crystalline bulk, perhaps under conditions of the glass transition or crystallization, can be the cause of spontaneous fibrillation of extrudates of liquid crystalline polymers. This instability results in the formation of fibrils of a certain size with interfaces. The easy formation of fibrils at lower ionic content may be explained by the domain flow and the instability of the TLCP bulk under the conditions of fiber drawing. In contrast, as the ionic content increases, more intermolecular interactions or ionic cross-links are formed, which may prevent the domain flow and reduce the instability of the TLCP bulk and, as a result, restrict the spontaneous fibrillation. More experimental observations and theoretical analysis will be needed to provide a more detailed explanation for the mechanism. Consistent with the DSC results, a multiphase feature has been observed for the 20 mol % ionic NTP sample, in which irregular domains are revealed in the micrograph (Figure 9c).

Lower magnification scans of fracture surfaces also show clear changes in fracture behavior with ionic content: at low ionic contents (1 and 2 mol %), fracture surfaces are not smooth, involving a layered structure or a macrofibril structure, which contain fibrils, reflecting

the crack propagation along the fiber axis to some degree in addition to the normal direction (Figure 8b). At higher ionic content levels (5, 7, and 10 mol %), such structures become less clear and the fracture surface becomes more flat, although there are still signs of crack propagation along the fiber direction (Figure 8c). Finally, at higher ionic contents (15 and 20 mol %), fracture surfaces become smooth (Figure 8d). Since less energy is consumed for crack propagation, which leads to smooth fracture surfaces, these fibers show more brittle behavior. These changes in fracture morphology are consistent with thermal behavior and optical textures: upon an increase in ionic monomer content, the molecular rigidity decreases, thus leading to reduced liquid crystallinity. This is reflected in less fibrous and more flat fracture surfaces. In addition, a higher degree of ionic interactions between polymer chains in samples of higher ionic contents causes less fibrillation by reducing the molecular alignment along the draw direction.

The skin surfaces of these fiber samples also exhibit interesting features, as shown by the SEM micrographs (see Figure 8). Because the fiber is drawn freely from the melt, its surface does not experience any confinement by other surfaces, and the appearance of its skin surface should represent characteristics of the polymer. A smooth surface with the skin being well-aligned along the long fiber axis is seen on the micrograph of the nonionic NTP sample (see Figure 8a). In contrast, all the ionic NTP samples exhibit a coarse skin surface with wavy bands roughly perpendicular to the long fiber axis. Although the cause of such structures is not clear, it



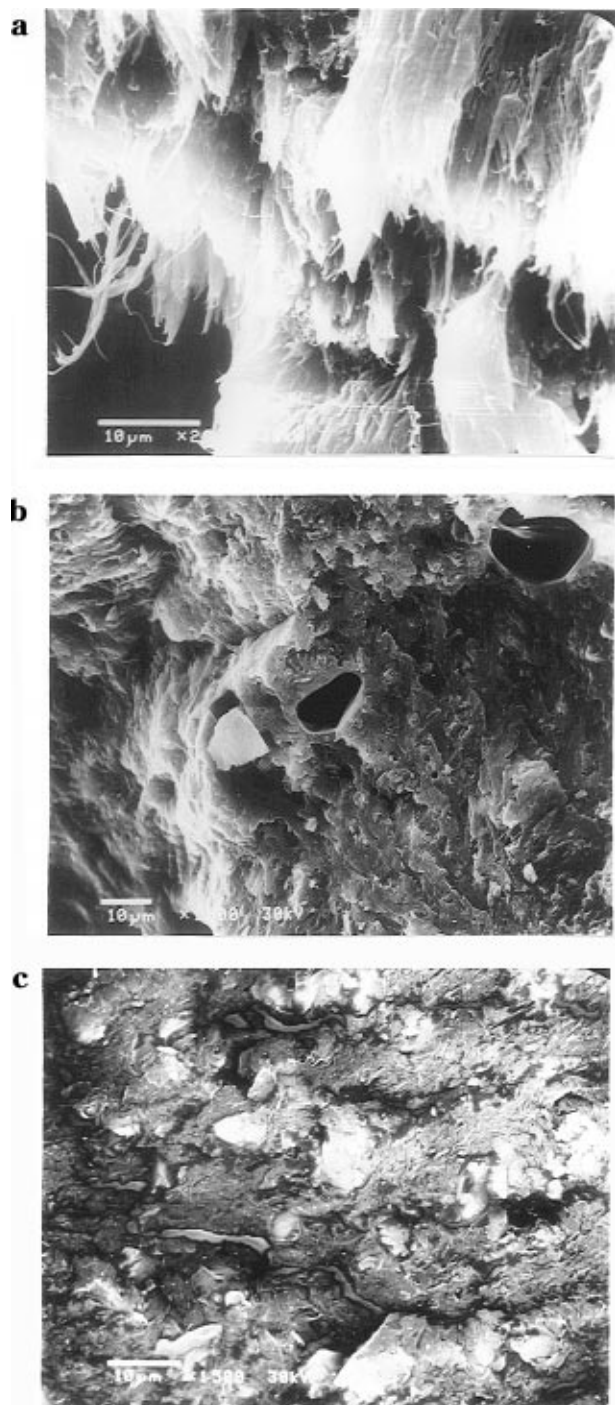


**Figure 9.** SEM micrographs at higher magnifications, revealing fracture surfaces of fibers: (a) 1 mol %; (b) 10 mol %; (c) 20 mol %.

should be related to the higher viscosity, although only qualitative observation was made at this time, and to larger intermolecular interactions found in ionic NTP samples. It should be added that such coarse features of surfaces can lead to better adhesion to other surfaces, such as found in fiber-reinforced composites.

## Conclusions

In this paper, a first report describing ionic NTPs, our major concerns are successful incorporation of proper amounts of ion-containing monomers into NTP chains and their general effects on thermal properties and morphologies of liquid crystalline polymers.

The meta-linked phenylene ring with an ionic group, sodium 5-sulfoisophthalate, is incorporated into the

NTP polymer based on HNA and HBA by melt acidolysis random copolymerization. Proper amounts of ionic groups are incorporated into the NTP polymer, as shown by IR spectroscopy and elemental analysis for representative ionic NTP samples. All the polymers prepared exhibit thermotropic liquid crystallinity: liquid crystalline mesophases are stable over a wide range of temperatures without transforming to the isotropic state at least up to 380 °C.

Overall changes in thermal properties are as follows. Nonionic NTP shows a sharp melting endotherm at 286 °C and no glass transition. Upon an increase in ionic content from 0 to 10 mol %, the degree of chain rigidity of the ionic NTP polymers decreases with ionic content: this is seen by a decrease in  $T_m$  (and  $T_i$ ) with ionic content and by an appearance of a glass transition (above 5 mol % ionic content) whose step becomes larger with ionic content. Upon a further increase in ionic content to 15 and 20 mol %, the crystalline (and melting) peaks become absent on DSC thermograms and the step of the glass transition is further increased. At 20 mol % ionic content, two glass transitions appear, which resemble the two glass transitions, reflecting a multiplet  $T_g$  and a cluster  $T_g$ , observed for conventional ionomers. Unlike conventional flexible ionomers whose glass transition temperatures increase with ionic content, the ionic NTP polymers show a relatively constant glass transition temperature below 10 mol % ionic content. This behavior is considered to be a result of the competition between two opposing factors: one is a "kinked" structure that reduces the rigidity of the polymer backbone chains, and another is an ionic interaction that restricts the segmental mobility of the polymer chain.

Birefringence is seen under crossed polarizers for all the ionic NTP samples. Fine scale threaded texture, characteristic to nematic LCPs, is observed: upon an increase in ionic content, the overall morphology changes from homogeneous to more heterogeneous structures, and eventually at high ionic contents of 15 and 20 mol %, more isotropic behavior is noted, although they still show birefringence. The changes in optical textures with the increase of ionic content may be related to the biphasic behavior of these ionic NTPs, arising from chemical heterogeneity due to random copolymerization.

The effect of ionic content on the fracture surface and skin surface morphology of the ionic NTP fibers was also observed. The degree of spontaneous fibrillation is reduced with an increase of ionic content, and it is suppressed when the ionic content reaches 7 mol %. Also, at high ionic content, fracture surfaces become more flat, reflecting less energy absorption during crack propagation, and thus more brittle behavior. The skin surfaces of all the ionic NTP fibers show coarse surfaces with wavy bands perpendicular to the long fiber axis, in contrast to the smooth skin surface of the nonionic NTP fiber. Such unique features should be related to the characteristics of ionic moieties attached to the polymer backbone, which may provide better adhesion properties, important in such materials as polymer blends and composites.

A study of ionic NTPs is useful not only for elucidating the effect of ionic interactions on the TLCPs, such as liquid crystalline morphology, spontaneous fibrillation, and thermal transitions, but also for developing novel TLCPs having excellent thermal and mechanical properties due to ionic bonds. The results on tensile and

compressive behavior of the ionic NTPs will be reported in the future.

Although the incorporation of meta-linked units reduces melting temperature, thus processing temperature, by over 70 deg, which is beneficial for processing, such units also introduce complexity: they reduce the rigidity of the polymer chains, resulting in, for example, decreased  $T_g$ , liquid crystallinity, and spontaneous fibrillation. This effect overlaps that of ionic interactions. To see the direct effect of ionic interactions on liquid crystalline behavior, it is better to eliminate this effect. This may be done by incorporating ionic "straight" units instead of "kinked" units. We are currently working on such a system, and results will be reported.

**Acknowledgment.** The authors would like to thank Drs. H. N. Yoon and J. P. Shepherd for useful discussions and W. Chen for help in initial synthesis work. We acknowledge Hoechst Celanese for support of this research. This research is also supported by the U.S. Army Research Office.

## References and Notes

- (1) Weiss, R. A.; Ober, C. K., Eds. *Liquid-crystalline polymers*; American Chemical Society: Washington, DC, 1990.
- (2) Donald, A. M.; Windle, A. H. *Liquid Crystalline Polymers*; Cambridge University Press: Cambridge, U.K., 1992.
- (3) Isayev, A. I.; Kyu, T.; Cheng, S. Z. D., Eds. *Liquid-Crystalline Polymer Systems*; ACS Symposium Series 632; American Chemical Society: Washington, DC, 1996.
- (4) Adams, W. W.; Eby, R. K. *MRS Bull.* **1987**, November, 22.
- (5) Kwolek, S. L. U.S. Pat. 1971, 3600350, assigned to E. I. du Pont de Nemours and Co.
- (6) Calundann, G. W. U.S. Pat. 1980, 4184996; 1981, 4256624, assigned to Celanese Co.
- (7) *Liquid Crystalline Polymer*; National Academy Press: Washington, DC, 1990.
- (8) Yoon, H. N.; Charbonneau, L. F.; Calundann, G. W. *Adv. Mater.* **1992**, 4 (3), 206.
- (9) Paul, D. R.; Newman, S. *Polymer Blends*; Academic Press: New York, 1978.
- (10) Olabisi, O.; Robeson, L. M.; Shaw, M. T. *Polymer-Polymer Miscibility*; Academic Press: New York, 1979.
- (11) Holliday, L. In *Ionic Polymers*; Holliday, L., Ed.; Applied Science: London, 1975; Chapter 1.
- (12) Eisenberg, A.; King, M. *Ion-Containing Polymers*; Academic Press: New York, 1977.
- (13) Hara, M.; Sauer, J. A. *J. Macromol. Sci., Rev. Macromol. Chem. Phys.* **1994**, C34, 325.
- (14) Smith, P.; Hara, M.; Eisenberg, A. In *Current Topics in Polymer Chemistry*; Ottenbrite, R. H.; Utracki, L. A.; Inoue, S., Eds.; Hanser Publishers: Munich, 1987.
- (15) Weiss, R. A.; Beretta, C.; Sasongko, S.; Garton, A. *J. Appl. Polym. Sci.* **1990**, 41, 91.
- (16) Molnar, A.; Eisenberg, A. *Macromolecules* **1992**, 25, 5774.
- (17) Douglas, E. P.; Sakurai, K.; MacKnight, W. J. *Macromolecules* **1991**, 24, 6776.
- (18) Calundann, G. W.; Jaffe, M. *Proc. Robert A. Welch Conf. Chem. Res.* **1982**, 26, 247.
- (19) Calundann, G. W. In *High Performance Polymers, Proceedings of the Symposium*; Seymour, R. B.; Kirshenbaum, G. S., Eds.; Elsevier: New York, 1986; p 235.
- (20) Romo-Uribe, A.; Windle, A. H. *Macromolecules* **1995**, 28, 7085.
- (21) Seo, Y.; Hong, S. M.; Hwang, S. S.; Park, T. S.; Kim, K. U.; Lee, S.; Lee, J. *Polymer* **1995**, 36, 515.
- (22) Yang, D.-K.; Krigbaum, W. R. *J. Polym. Sci., Polym. Phys. Ed.* **1989**, 27, 819.
- (23) Kaito, A.; Kyotani, M.; Nakayama, K. *Macromolecules* **1990**, 23, 1035.
- (24) Yoon, H. N. *Colloid Polym. Sci.* **1990**, 268, 230.
- (25) Shepherd, J. P.; Farrow, G.; Wissbrun, F. U.S. Pat. 1993, 5227456, assigned to Hoechst Celanese Co.
- (26) Xue, Y.; Hara, M. To be submitted for publication.
- (27) Xue, Y.; Hara, M. To be submitted for publication.
- (28) Noda, I.; Dowrey, A. E.; Marcott, C. In *Physical Properties of Polymers Handbook*; Mark, J. E., Ed.; AIP Press: New York, 1996; Chapter 21.
- (29) Kaito, A.; Kyotani, M.; Nakayama, K. *Macromolecules* **1991**, 24, 3244.
- (30) Yi, X.-S.; Zhao, G.; Shi, F. *Polym. Int.* **1996**, 39, 11.
- (31) Sakurai, K.; Douglas, E. P.; MacKnight, W. J. *Macromolecules* **1993**, 26, 208.
- (32) Sakurai, K.; Douglas, E. P.; MacKnight, W. J. *Macromolecules* **1992**, 25, 4506.
- (33) Nakanishi, K. In *Infrared Absorption Spectroscopy (Practical)*; Holden-Day Inc.: San Francisco, 1962; p 54.
- (34) Daniels, W. W.; Kitson, R. E. *J. Polym. Sci.* **1958**, 33, 161.
- (35) Fadini, A.; Schnepel, F.-M. *Vibrational Spectroscopy*; Ellis Horwood Ltd.: New York, 1989; p 67.
- (36) Longworth, R. In *Ionic Polymers*; Holliday, L., Ed.; Applied Science: London, 1975; Chapter 2.
- (37) Rees, R. W. In *Polyelectrolytes*; Frish, K. C.; Klempner, D.; Patsis, A. V., Eds.; Technomic Publishing: Westport, CT, 1976; p 177.
- (38) Siemionko, R. K. U.S. Pat. 1983, 4370466, assigned to E. I. du Pont de Nemours and Co.
- (39) Hanna, S. Ph.D. Thesis, Cambridge University, 1989. Reference 2, p 165.
- (40) Ma, X.; Sauer, J. A.; Hara, M. *Macromolecules* **1995**, 28, 3953.
- (41) Hird, B.; Eisenberg, A. *Macromolecules* **1992**, 25, 6466.
- (42) Eisenberg, A.; Hird, B.; Moore, R. B. *Macromolecules* **1990**, 23, 4098.
- (43) Sawyer, L. C.; Grubb, D. T. In *Polymer Microscopy*; Chapman and Hall: New York, 1987; p 241.
- (44) Due to the limitation of the heating unit, 380 °C is the highest temperature reached in our experiments. This is also close to the degradation temperature, determined by TGA, for most of the ionic NTP samples.
- (45) Thomas, E. L.; Wood, B. A. *Faraday Discuss. Chem. Soc.* **1985**, 79, 229.
- (46) Viney, C.; Donald, A. M.; Windle, A. H. *J. Mater. Sci.* **1983**, 18, 1136.
- (47) D'Allest, J. F.; Sixou, P.; Blumstein, A.; Blumstein, R. B. *Mol. Cryst. Liq. Cryst.* **1988**, 157, 229.
- (48) Martin, P. G.; Stupp, S. I. *Macromolecules* **1988**, 21, 1222.
- (49) Weinkauff, D. H.; Paul, D. R. *J. Polym. Sci., Polym. Phys. Ed.* **1992**, 30, 837.
- (50) Baer, E.; Hiltner, A.; Weng, T.; Sawyer, L. C.; Jaffe, M. *Polym. Mater. Sci. Eng.* **1985**, 52, 88.
- (51) Weng, T.; Hiltner, A.; Baer, E. *J. Mater. Sci.* **1986**, 21, 744.
- (52) Sawyer, L. C.; Jaffe, M. *J. Mater. Sci.* **1986**, 21, 1897.
- (53) Plate, N. A. In *Liquid-Crystal Polymers*; Plate, N. A., Ed.; Plenum Press: New York, 1993; p 422.

MA961703X